Clim Dyn
DOI 10.1007/s00382-014-2301-7

Effects of cumulus parameterizations on predictions of summer flood in the Central United States

Fengxue Qiao · Xin-Zhong Liang

Received: 16 May 2014 / Accepted: 12 August 2014

Abstract This study comprehensively evaluates the effects of twelve cumulus parameterization (CUP) schemes on simulations of 1993 and 2008 Central US summer floods using the regional climate-weather research and forecasting model. The CUP schemes have distinct skills in predicting the summer mean pattern, daily rainfall frequency and precipitation diurnal cycle. Most CUP schemes largely underestimate the magnitude of Central US floods, but three schemes including the ensemble cumulus parameterization (ECP), the Grell-3 ensemble cumulus parameterization (G3) and Zhang-McFarlane-Liang cumulus parameterization (ZML) show clear advantages over others in reproducing both floods location and amount. In particular, the ECP scheme with the moisture convergence closure over land and cloud-base vertical velocity closure over oceans not only reduces the wet biases in the G3 and ZML schemes along the US coastal oceans, but also accurately reproduces the Central US daily precipitation variation and frequency distribution. The Grell (GR) scheme shows superiority in reproducing the Central US nocturnal rainfall maxima, but others generally fail. This advantage of GR scheme is primarily due to its closure assumption in which the convection is determined by the tendency of large-scale instability. Future study will attempt to incorporate the large-scale tendency assumption as a trigger function in the ECP scheme to improve its prediction of Central US rainfall diurnal cycle.

Keywords Cumulus parameterization · Regional climate model · Extreme events · Diurnal cycle · Frequency distribution

1 Introduction

The Central United States is the world's most productive, agriculture region. During the summer, heavy rainfall events frequently occur over this region and cause severe floods with devastating damages and considerable socio-economic consequences (Kunkel et al. 1994; Smith et al. 2013; Nakamura et al. 2013). These extreme heavy rainfall events have been identified with complicated physical mechanisms at different scales. They include large-scale circulation anomalies (Bell and Janowiak 1995; Mo et al. 1997), the sub-continental moisture transport from the Great Plain low-level jet (Mo et al. 1997; Ting and Wang 2006), and the remote supplies from the Caribbean region (Dirmeyer and Kinter 2010), as well as the local effects of land surface processes (Beljaars et al. 1996; Paegle et al. 1996; Bosilovich and Sun 1999). Therefore, summer floods over the Central US provide an ideal test for evaluation of physical process representations in regional climate models (RCMs).

However, it is still a great challenge for most RCMs to make accurate prediction of precipitation at relatively flat

F. Qiao
Key Laboratory of Geographic Information Science, Ministry of Education, East China Normal University, Shanghai, China

F. Qiao · X.-Z. Liang
Department of Atmospheric Sciences, University of Illinois at Urbana–Champaign, Urbana, IL, USA

X.-Z. Liang (✉)
Earth System Science Interdisciplinary Center, University of Maryland, 5825 University Research Court, Suite 4001, College Park, MD 20740, USA
e-mail: xliang@umd.edu

X.-Z. Liang
Department of Atmospheric and Oceanic Science, University of Maryland at College Park, College Park, MD, USA

Published online: 26 August 2014

region such as the Central US (Takle et al. 1999; Liang et al. 2012), especially during summer when moist convective systems prevail (Liang et al. 2001, 2004b). Most studies have suggested that systematic errors still exist in predicting the Central US summer precipitation and large uncertainties are associated with the choice of CUPs, regarding the rainfall amount (e.g., Liang et al. 2004b, 2006, 2007, 2012), daily precipitation frequency and intensity (e.g., Liang et al. 2006), and the rainfall diurnal cycle (e.g., Dai 1999; Davis et al. 2003; Liang et al. 2004a; Lee et al. 2007b, 2008).

For instance, Anderson et al. (2003) compared the simulations of 1993 summer flood from 13 RCMs and found all underestimate the maximum rainfall intensity and unrealistically produce the heaviest rainfall northeast of the observed flooding center. Liang et al. (2004b) showed that the cumulus parameterization of Grell (1993) scheme and Kain and Fritsch (1993) complementarily capture the summer rainfall distribution over the Central and Southeast US Specifically, the Kain-Fritsch scheme yields excessive rainfall in the Southeast, but large deficits over the Central US, while the Grell scheme better captures the rainfall amount over the Central US but with great underestimations over the Southeast US.

Although the model sensitivity to CUPs has been widely recognized regarding summer rainfall prediction, it is still not entirely clear about the CUP effects because these studies were generally based on different models and/or focused on a few CUPs included in RCMs. As numerous cumulus parameterizations are available in current numerical weather/climate models, it has become a challenge for weather forecasters or climate researchers to properly select CUPs for accurate predictions, especially for summer rainfall extremes. Hence, it is important to systematically evaluate the relative performance of a large suite of the most common CUPs using fully-developed RCMs focusing on their effects on summer rainfall prediction.

Regarding the prediction of daily rainfall frequency distribution, previous studies mainly focused on the occurrence of heavy rainfall events which are essential to climate impacts assessments (Liang et al. 2006). Many studies examined the observed changes of extreme rainfall events and showed the frequency of heavy rainfall events has increased during the recent decades over the Central US (Karl and Knight 1998; Kunkel et al. 2003; Villarini et al. 2011; Groisman et al. 2012). However, difficulties still existed for most RCMs (e.g., Liang et al. 2006) in predicting the observed daily rainfall frequency. They generally overestimate the number of dry days, but underestimate the heavy rainfall occurrence. This model failure has been identified with the problem of CUPs in which convection was initiated too often with weak convective available potential energy (CAPE) accumulations (Dai 1999; Liang et al. 2006).

Another long-standing problem is the accurate prediction of the observed nocturnal rainfall maxima over the Central US (e.g., Lee et al. 2007a; Trenberth et al. 2003). Most studies have also ascribed this difficulty to the CUP problem in which moist convection is too strongly coupled with surface forcing and thus lacks sensitivity to large-scale dynamic forcing (e.g., Dai 1999; Lee et al. 2007a). However, a few CUPs were found to be able to capture the nocturnal rainfall maxima, such as the Grell (1993) cumulus scheme (Liang et al. 2004a) and the simplified Arakawa-Schubert (Pan and Wu 1995) scheme (Lee et al. 2008). It is imperative to examine whether the superiority of these schemes exist in different RCMs and what are the primary causes for their success, separating relative contributions from closure assumption or trigger function.

The regional climate-weather research and forecasting model (CWRF) incorporates the most comprehensive list of CUPs that have been widely used in both regional and global climate models (Liang et al. 2012). This study will base on CWRF simulations to provide a consistent rigorous evaluation of various CUPs in predicting the Central US summer floods with respect to three key characteristics: mean amount and pattern, daily frequency distribution and the diurnal cycle. The main objective is to identify the strength and weakness of individual CUP schemes. This paper is organized as follows. Section 2 describes the CWRF model physical configurations and gives a summary of CUP schemes incorporated in the CWRF, as well as the observational precipitation data used for model verification. Section 3 lists four sets of experiments. The major results are presented in Sect. 4, 5, and 6. Section 7 summarizes the conclusion and discussion.

2 Model description, cumulus schemes and observations

2.1 Model configuration

The CWRF model has been developed from the Weather Research and Forecasting model v3.1.1 (WRF, Skamarock et al. 2008) with numerous improvements of physical processes that are essential to climate scales, including the interaction between land–atmosphere–ocean, convection-microphysics and cloud-aerosol-radiation (Liang et al. 2012). More details about the CWRF default model physical configuration can be referred to Liang et al. (2012). For this study, all the model experiments are based on the default physics configuration of the CWRF (Liang et al. 2012). This includes the Conjunctive Surface–Subsurface Process Model (CSSP) for land surface scheme, and the NASA Goddard Space Flight Center (GSFC) scheme for the radiation scheme.

The CSSP scheme is a newly developed scheme in CWRF. It is the core land surface model to predict soil temperature/moisture distributions, terrestrial hydrology variations, and land–atmosphere flux exchanges. It has significant improvements in representing surface energy and hydrology processes, including an improved dynamics-statistical parameterization of land surface albedo (Liang et al. 2005), a 3-D subsurface hydrologic model with a scalable representation of subgrid topographic control on soil moisture (Choi et al. 2007) and an explicit treatment of surface–subsurface flow interaction (Choi and Liang 2010; Yuan and Liang 2011; Choi et al. 2013).

The GSFC radiation package includes the parameterizations developed by Chou and Suarez (1999) for shortwave and by Chou et al. (2001) for longwave radiation. It is not the scheme included in WRF, but was first implemented into CWRF by Liang and later as an integral part of the Cloud-Aerosol-Radiation ensemble system (CAR, Liang and Zhang 2013). It accounts for the radiative effects of long-lived greenhouse gases (CO_2, CH_4, N_2O, CFCs) of the present-day volume mixing ratios, as well as O3 and aerosol distributions. By default, CAR specifies daily O3 3-D distributions via interpolation from the monthly climatology based on satellite and ozonesonde measurements (Liang et al. 1997), and daily aerosols as defined by their optical depth and single-scattering albedo geographic distributions from the MISR satellite retrievals (Kahn et al. 2007) with certain vertical scaling. It also incorporates the radiative effect of clouds using fractional cover scheme of Xu and Randall (1996) and optical properties depending on hydrometeors as in Liang et al. (2004b).

The CWRF computation domain is centered at (37.5°N, 95.5°W) using the Lambert conformal map projection. It covers the whole continental US and adjacent ocean with 30-km horizontal grid spacing, including the total grid points of 197 (west–east) × 139 (south–north). There are 36 vertical levels with refined resolutions near the surface to improve the planetary boundary layer (PBL) and convection representation, and around the melting altitude (~800–650 hPa) to better simulate the cloud microphysics processes.

The initial atmosphere, surface states and time-varying lateral boundary conditions for CWRF are given by the European Centre for Medium-Range Weather Forecasts (ECMWF) Interim Reanalysis (ERI, Uppala et al. 2008). The ERI data are available at 6 hourly intervals with 1.5° horizontal grid spacing.

2.2 Cumulus parameterization

The CWRF model incorporates 7 new cumulus parameterizations (ZML, CSU, GFDL, MIT, GR, ECP, UW), in addition to the 7 original WRF schemes (BMJ, NKF, SAS, NSAS, TDK, GD, G3). All these CUP schemes by above abbreviations are defined in Table 1 with respective references. They are built to predict surface total precipitation rates, cloud base and top levels, and vertical atmospheric heating and moistening profiles. Some include additional output such as wind tendencies or convective in-cloud liquid or ice water profiles, which are also listed in the Table 1. To consistently evaluate the effects of deep cumulus schemes, shallow cumulus parameterization internally built in 8 CUPs (BMJ, NKF, SAS, NSAS, TDK, ZML, G3, and ECP) are switched off but all coupled with the single UW shallow scheme. According to the fundamental closure assumption in the CUP, these deep and shallow cumulus schemes can be generally divided into three categories: (1) Multiple closures (ECP, G3, and GD); (2) Total instability adjustment closure (ZML, NKF, and TDK); (3) Quasi-equilibrium closure-based (BMJ, GR, MIT, GFDL, SAS, NSAS, CSU). The major assumptions and specific features for each category are further illustrated in the Appendix 1.

2.3 Verification data

Several major daily precipitation datasets are utilized for precipitation verification over the continental US and Northern Mexico. The primary one is constructed from rain gauge measurements from 7,235 stations over the continental US and adjusted by the monthly mean of PRISM (Parameter-elevation Regression on Independent Slopes Model, Daly et al. 2008) for the statistical topography-precipitation relationships particularly important over the western US mountain regions (Liang et al. 2004b). Another one is derived from the National Oceanic and Atmospheric Administration Climate Prediction Center (CPC) global 0.5° analysis of daily gauge measurements (Chen et al. 2008) to supplement data over Canada and Mexico. The 3-hourly fine-resolution (32 km) North American Regional Reanalysis (NARR) will be utilized to evaluate the diurnal cycle simulations. This NARR 3-hourly precipitation are determined by the Eta Model coupled with a 3D variational data assimilation system that integrates observations including the 1/8° rain gauge analysis over the continental US, and the 1° rain gauge analysis for Mexico and Canada, as well as the 2.5° global analysis from the CPC merged analysis of precipitation over oceans and land south of Mexico (Mesinger et al. 2006). It has been widely applied in model verification and diagnostic studies for its advantages in replicating the continental US precipitation features, especially the diurnal variations (Jiang et al. 2006; Becker and Berbery 2008).

The observational precipitation data over oceans are also included for a basic evaluation of CUP effects over the US coastal oceans. After the year of 1998, the Tropical Rainfall Measuring Mission (TRMM) 3-hourly and daily

Table 1 A summary of CWRF cumulus parameterization schemes with the related references

CUP	References	Closure	Trigger	Momentum tendencies	Moisture tendencies	Shallow
ECP	Modified from G3 (Liang et al. 2012; Qiao and Liang 2014a, b)	Multiple	Maximum cap strength	No	Qc, Qi	Yes
G3	Grell and Dévényi (2002)	Multiple without QE	Maximum cap strength	No	Qc, Qi	Yes
GD	Grell and Dévényi (2002)	Multiple	Maximum cap strength	No	Qc, Qi	No
ZML	Zhang and McFarlane (1995)	Total instability adjustment	CAPE > 0	Yes	Qc, Qi	No
NKF	Kain and Fritsch (1993), Kain (2004)	Total instability adjustment	CAPE > 0; Parcel temperature perturbation	No	Qc, Qi, Qr, Qs	Yes
TDK	Tiedtke (1989), Nordeng (1995)	Total instability adjustment	Moisture convergence	Yes	Qc, Qi	Yes
BMJ	Betts and Miller (1986), Janjic (1994)	QE assumption	Positive cloud work function threshold	No	–	Yes
GR	Grell (1993)	QE assumption (instability tendency)	Lifting depth trigger	No	–	No
MIT	Emanuel and Živković-Rothman (1999)	Subcloud layer-based QE assumption	Environment is unstable to a parcel	Yes	–	No
GFDL	Donner (1993), Donner et al. (2001)	QE assumption	CAPE > 0; ΔCAPE > 0	No	Qc, Qi	No
SAS	Pan and Wu (1995)	QE assumption	Critical cloud work function; Lifting depth trigger	Yes	Qc, Qi	Yes
NSAS	Han and Pan (2011)	QE assumption	Lifting depth trigger	Yes	Qc, Qi	Yes
CSU	Fowler and Randall (2002)	QE assumption (prognostic CKE)	CKE dissipation rate	No	Qc, Qi, Qr, Qs	No
UW	Bretherton and Park (2009)	Subcloud layer-based QE	Turbulent kinetic energy	Yes	Qc, Qi, Qr, Qs	Yes

Qc, Qi, Qr, Qs: mixing ratio of cloud water, ice, rain, and snow

product (3B42 version 7, 50° S–50° N, 0.25° × 0.25° grids, 1998–2009) is mapped onto the CWRF 30 km-grids using bilinear spatial interpolation to increase the comparability with model simulation. In addition, the coarse-resolution monthly data from the CPC Merged Analysis of Precipitation (Xie and Arkin 1997) are used before the 1998 when the TRMM data is not available. All these observational data sets are summarized in Table 2.

3 Model experiment design

Table 3 lists five sets of sensitivity experiments conducted for this study, including their different physical configurations and study objectives:

1. The first set of experiments uses the CWRF model with 12 individual CUP schemes to conduct integrations from May 1 to August 31 for 1993 and 2008 when both record floods occurred over the Central US (Dirmeyer and Kinter 2010). Among the 14 CUP schemes in CWRF, the UW scheme is utilized as a common shallow convection option and the GD scheme is eliminated by its successor G3 scheme, and thus only 12 remaining CUP schemes are evaluated regarding the predictions of key precipitation features over the Central US.

As shown below, only the GR cumulus scheme is able to capture the nocturnal rainfall signal over the Central US. Therefore, four additional sensitivity experiments are conducted below to address issues related to the superiority of the GR scheme.

2. The second set of experiments compares the CWRF diurnal simulations with and without GR cumulus scheme in order to examine the role of GR scheme in regulating the rainfall diurnal cycle over the Central US. The experiment "No CUP" means the CWRF simulation using the default physics configuration except that the cumulus parameterization was deactivated. It can be used to examine the effects of cumulus parameterization on total rainfall prediction.
3. The third set of experiments uses GR cumulus scheme combining with three different microphysics schemes, aiming at investigating whether the superiority of GR cumulus scheme is affected by the representation of large-scale microphysics. Three cloud microphysical parameterizations include the Goddard Cumulus Ensemble (GCE) model (Tao et al. 2003), the New

Table 2 A summary of observational data sets used for model verification

Data set	Spatial resolution	Temporal resolution	Strengths/weaknesses
Rain gauge measurements from 7,235 National Weather Service cooperative stations over the US (Liang et al. 2004b)	Mapped onto the CWRF grid with 30 km grid spacings	Daily (1979–2008)	Station density is high and compatible with the CWRF 30-km grid except for mountainous regions in the Rockies
PRISM (Daly et al. 2008)	0.04° × 0.04° over the US	Monthly (1979-present)	Adjust the rain gauge measurements for the terrain dependence over the western US mountainous regions by adding the statistical topography-precipitation relationships (Liang et al. 2004a, b)
CPC global gauge measurements (Chen et al. 2008)	0.5° × 0.5° global	Daily (1948–2006)	Supplement data over the Canada and Mexico that are not available in the primary US rain gauge dataset
NARR (Mesinger et al. 2006)	32 km over the US	3-hourly (1979–2013)	Widely applied in model verification and diagnostic studies for its advantages in replicating the continental US precipitation diurnal variations (Jiang et al. 2006; Becker and Berbery 2008)
TRMM (3B42 version 7)	0.25° × 0.25° 50°S–50°N	3-hourly (1998-present)	Supplement data over the US coastal oceans, available only after 1998
CMAP (Xie and Arkin 1997)	2.5° × 2.5° global	Monthly (1979–2011)	Supplement data over the US coastal oceans before 1998 when the TRMM data was not available

Thompson (Thompson et al. 2008), and the Morrison et al. (2009) scheme. A brief description of these three popular microphysics schemes is given in the Appendix 2.

4. Given that the ECP scheme includes five cumulus closure assumptions (AS, W, MC, KF, and TD, in Appendix 1), the fourth set of experiments attempt to explore the effects of these five closures on the Central US diurnal cycle simulation, emphasizing on the TD closure that is also used by the GR cumulus scheme. The results can help explain the contribution of closure assumption in controlling the diurnal cycle that is successfully simulated by GR cumulus scheme.
5. Motivated by the study of Lee et al. (2008) in which the lifting depth trigger plays a key role on the realistic simulation of summer rainfall diurnal phase over the Central US, the last set of experiments uses the GR scheme with different lifting depth triggers. The comparative studies among the last two groups of experiments help identify which component(s) in the CUPs are more critical for capturing the nocturnal rainfall maximum over the Central US.

4 Summer mean precipitation amount and pattern

The two summer floods occurring in the 1993 and 2008 both affected the vast areas of the Central US and caused comparably severe damages and large economic lost (Coleman and Budikova 2010). The following comparisons are made on the main flooding periods of 1993 JJA (June–August) and 2008MJJ (May–July) to systematically depict the model sensitivity to the convective parameterization. Figure 1 demonstrates the geographic distributions of observed and CWRF simulated 1993 summer mean precipitation by using 12 different CUP schemes including the ECP, G3, BMJ, ZML, NKF, TDK, GR, MIT, GFDL, SAS, NSAS and CSU. Several model deficiencies can be identified in the major rainfall areas.

First, all CUP schemes produce a heavy rainfall center over the Central US with large discrepancies in the simulated rainfall amounts. The ECP, G3, and ZML show clear advantages over other schemes in reproducing the floods location and amount. However, most CUP schemes that originally developed and often used in coarse-resolution GCMs, such as TDK, MIT, GFDL and CSU, systematically underestimate the summer rainfall amount over the Central US. This suggests that further refinements are required to account for the scale dependence of CUP in weather prediction and climate simulation.

Second, three schemes such as the G3, ZML, and NKF produce widespread large wet biases along the US Atlantic coast oceans. In particular, the ZML significantly

Table 3 Summary of four groups of sensitivity experiments conducted by CWRF with different cumulus and microphysics configurations

Sensitivity experiments	Integration time	Deep CUP	Microphysics
1. CUP test	1993 May 1–August 31 2008 May 1–August 31	12 CUPs [ECP, G3, BMJ, ZML, NKF, TDK, GR, MIT, GFDL, SAS, NSAS, CSU]	GCE
2. GR test	1993 May 1–August 31	No CUP Grell	GCE
3. MP test	1993 May 1–August 31	Grell	GCE New Thompson Morrison
4. Closure test	1993 May 1–August 31	ECP [AS, W, MC, KF, TD closures]	GCE
5. Trigger test	1993 May 1–August 31	Grell [three lifting depth triggers]	GCE

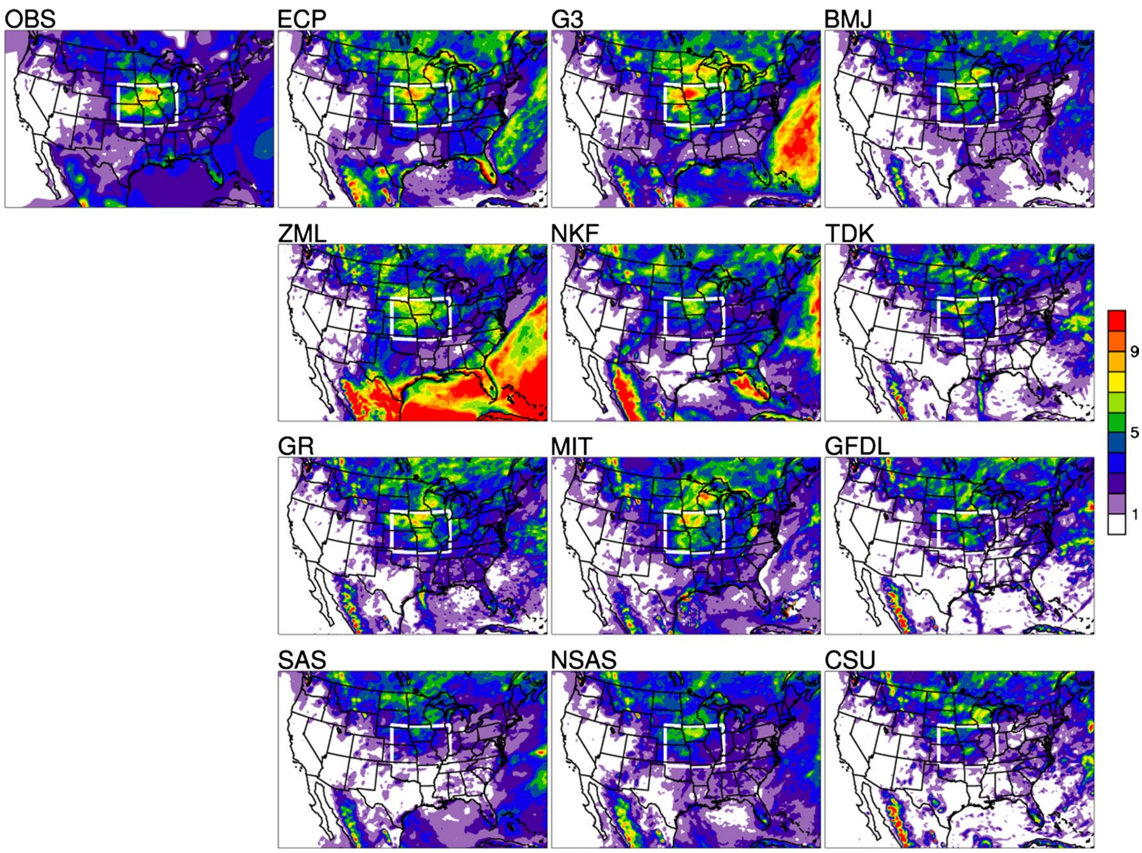

Fig. 1 The geographic distributions of observed and simulated 1993 summer mean precipitation by the CWRF using 12 different cumulus parameterization schemes including the ECP, G3, BMJ, ZML, NKF, TDK, GR, MIT, GFDL, SAS, NSAS and CSU. *Outlined white boxes* are the Central US for the flooding area of interest (36°–43°N, 100°–87°W)

overestimates the summer mean precipitation over the entire US East plus South Coast oceans. The ECP scheme is developed from the G3 scheme, but more realistically simulates the rainfall pattern and intensity along the US Atlantic Coast than the G3 scheme. The main reason is that the ECP only adopts the cloud-base vertical velocity closure instead of the ensemble of multiple closures in the G3 scheme. On the other hand, the ZML and NKF both based on the total instability removal closure assumption generally yield excessive coastal ocean rainfall amounts. This is consistent with the previous finding of Liang et al. (2004b) that Kain and Fritsch (1993) scheme using that closure produced large wet bias along the US coast oceans. However, the TDK scheme using a similar total instability removal closure does not produce large wet biases as the ZML and NKF schemes do. This may suggest the compensating effects from differences in trigger functions, for which the TDK scheme uses the moisture convergence, while the other two schemes use the positive convective instability.

Figure 2 summarizes the CWRF simulated mean rainfall biases compared to the observations averaged over the

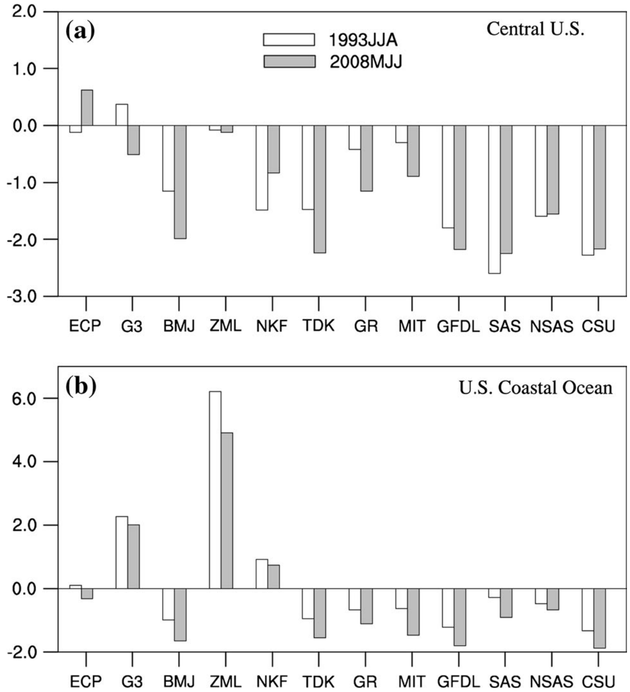

Fig. 2 The mean precipitation biases simulated by the CWRF using the 12 different cumulus schemes from the observations averaged over the Central US (**a**) and the US Atlantic Coast and Gulf of Mexico (**b**) for 1993 June–August and 2008 May–July

Central US and the US Atlantic Coast plus Gulf of Mexico for 1993 JJA and 2008 MJJ by using the 12 different CUPs. Combined with the mean bias statistics in Table 4, the result clearly shows that ZML produces the smallest biases over the Central US for both cases, but significantly overestimates the rainfall along the US coastal oceans. The ECP and G3 schemes both generate smaller biases over the Central US, but ECP greatly reduces the G3 wet biases along the US coastal oceans. To evaluate the CUP performances in predicting the general pattern of summer mean precipitation, Table 4 also compares the pattern correlation coefficients and root-mean-square (RMS) errors of summer mean precipitation between observations and CWRF simulations using 12 CUP schemes for both 1993 and 2008 cases over the continental US. It shows that six schemes, including ECP, G3, BMJ, GR, MIT, and NSAS, have advantages over others in reproducing summer mean precipitation across the entire contiguous US. The outlier is ZML which produces the overall lowest geographic pattern correlation and highest RMS errors for the summer mean rainfall amount.

The above comparisons indicate that predictive skills of different CUP schemes with respect to the summer mean precipitation are strongly dependent upon climate regimes. Three schemes including ECP, G3 and ZML produce relatively smaller mean biases over the Central US than other schemes, while G3 produces large wet biases over the US coastal oceans, and ZML has worst performance in predicting the overall pattern distribution due to the wet biases over the North American monsoon region and Southeast US coastlines. In contrast, the BMJ, GR, MIT and NSAS show advantages over others in simulating the general pattern of summer mean precipitation in the entire contiguous US but they tend to have large deficits over the Central US.

Given the complementary regime-dependences of these seven schemes (ECP, G3, ZML, BMJ, GR, MIT, NSAS) in model predictions of summer mean rainfall distributions, the following two sections will focus on these schemes to evaluate their relative performances in predicting the daily rainfall features and diurnal cycle over the Central US.

Table 4 CWRF simulated rainfall statistics for 1993 JJA (June–August) and 2008 MJJ (May–July) by using 12 different cumulus parameterization schemes

CUPs	Bias (%) [Central US]		Pattern correlation (US)		RMS errors (US)		Daily rainfall correlation (Central US)		Normalized variances (Central US)	
	1993	2008	1993	2008	1993	2008	1993	2008	1993	2008
ECP	**−2.4**	**13.7**	**0.69**	**0.74**	**1.70**	**1.77**	**0.65**	**0.65**	**1.11**	**1.16**
G3	**7.1**	**−11.3**	**0.71**	**0.72**	**1.57**	**1.28**	**0.65**	**0.60**	**1.29**	**1.01**
BMJ	−21.9	−43.5	**0.71**	**0.67**	**1.35**	**1.25**	0.58	0.52	0.89	0.51
ZML	**−1.6**	**−2.7**	0.41	0.54	2.91	2.45	0.59	0.50	1.23	0.82
NKF	−28.6	−18.1	0.59	0.67	1.96	1.42	0.50	0.54	0.99	1.00
TDK	−28.4	−49.0	0.64	0.60	1.64	1.45	0.44	0.48	1.25	0.74
GR	−8.1	−25.2	**0.72**	**0.71**	**1.38**	**1.17**	0.43	0.53	1.33	0.85
MIT	−5.8	−19.5	**0.68**	**0.69**	**1.46**	**1.28**	0.51	0.47	1.10	0.96
GFDL	−34.6	−47.6	0.61	0.62	1.76	1.43	0.39	0.48	1.06	0.66
SAS	−49.8	−49.1	0.61	0.65	1.63	1.33	0.39	0.48	0.56	0.68
NSAS	−30.7	−34.1	**0.69**	**0.69**	**1.31**	**1.15**	**0.62**	**0.61**	**0.73**	**0.58**
CSU	−43.8	−47.5	0.54	0.61	1.92	1.44	0.43	0.51	0.76	0.69

The bold numbers demonstrate the respective advantages of seven schemes (ECP, G3,ZML, BMJ, GR, MIT, NSAS) in predicting the general summer mean pattern/amount over the entire continental US and daily rainfall variations in the Central US

5 Daily precipitation variation and frequency distribution

Figure 3 compares the model results with observations for both 1993 and 2008 floods in Taylor diagrams (Taylor 2001) by depicting three important statistics based on daily precipitation averaged over the central US: temporal correlation, normalized standard deviation, and RMS errors. The cosine of the angle of model points from the horizontal axis represents the temporal correlation with observations. The radial coordinate depicts the normalized variances which is the ratio of the modeled to observed standard deviation. It indicates the relative amplitude of model and observed variations. The RMS difference between the model and observation is proportional to the linear distance between the model point and the "REF" point lying on the horizontal axis. The plotted values in the diagrams are also listed in Table 4 for reference.

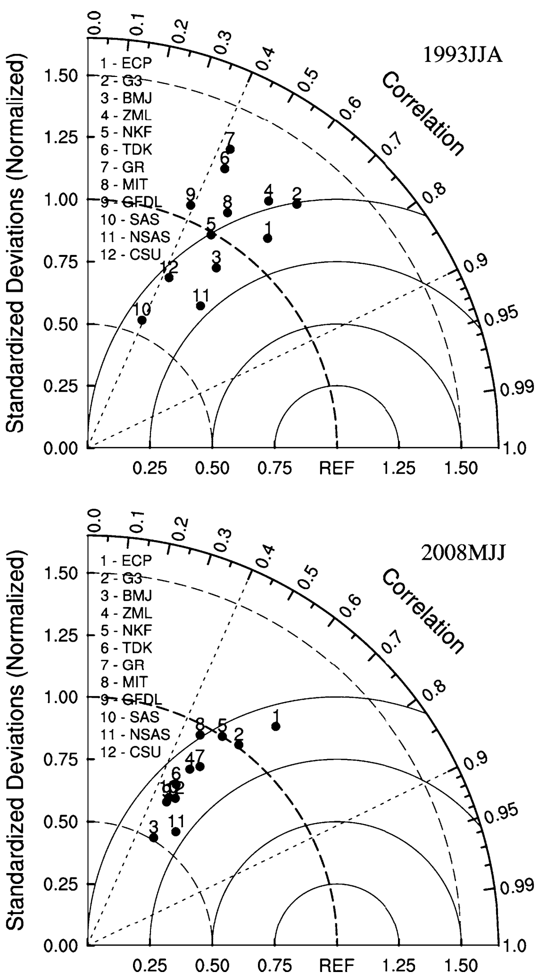

Fig. 3 Taylor diagram showing the model performance of simulated 1993 JJA (June–August) and 2008 MJJ (May–July) daily precipitation variability averaged over the Central US by using 12 different cumulus parameterization schemes, in terms of the normalized standard deviation of the modeled daily means (proportional to the distance from the origin), the RMS difference between the simulated and observed daily means (proportional to the distance from the REF point), and the temporal correlation between the simulated and observed daily means (cosine values of the angle of model point from the horizontal axis)

Among all the CUP schemes over the Central US, ECP produces the highest temporal correlations (0.65, 0.65) and small normalized variance (1.11, 1.16) for both cases, indicating its superiority in reproducing the daily rainfall variations. Although G3 (0.65, 0.60) and NSAS (0.62, 0.61) both well capture the temporal correlation, G3 generates relatively larger normalized variance (1.29, 1.01) than ECP especially for 1993 flood, and NSAS significantly underestimates the amplitude of daily variation (0.73, 0.58). On the other hand, ZML poorly simulates the daily rainfall variation (0.59, 0.50), albeit with the smallest mean biases (−1.6, −2.7 %).

Several widely-used CUP schemes show advantages in reproducing the general spatial patterns of summer mean precipitation over the entire continental US for both cases, including ECP, G3, BMJ, GR, MIT, NSAS, but with large spread of the RMS errors for the summer mean rainfall amounts. Among these five schemes, most of them consistently produce the dry biases over the Central US. For instance, BMJ largely underestimates the summer floods for both cases (−21.9, −43.5), GR produces great underestimations (−8.1, −25.2), and NSAS even reaches −30.7 and −34.1 for both cases. Therefore, ECP and G3 are the two schemes that best capture the summer mean pattern and amounts of rainfall over the entire continental US.

Figure 4 compares the frequency distributions of 1993 summer daily precipitation and relative contributions from each daily precipitation rate bin to the total amount over the Central US between the observations, the ERI reanalysis, and CWRF simulations with the aforementioned seven CUP schemes. Here, the observations are daily precipitation data from the rain gauge measurements adjusted by the monthly mean PRISM (details in Table 2). The range of daily precipitation intensity is divided into 1 mm/day bins from 0 to 50 mm day-1 and the frequency distribution at each bin counts all the grids within the Central US without spatial and temporal average. The 2008 case (not shown) exhibits the similar characteristics. The ERI reanalysis systematically overpredicts the occurrence and contribution of light rainfall events with daily intensity less than 10 mm day-1, but significantly underestimates the frequency and intensity of extreme events with daily rainfall exceeding 35 mm day-1. The seven CUP schemes can be roughly divided into two groups according to their daily rainfall frequency predictions. One group, including ECP, G3, and ZML schemes, more realistically reproduce the overall frequency distribution by greatly reducing the ERI deficiency in predicting the heavy rainfall

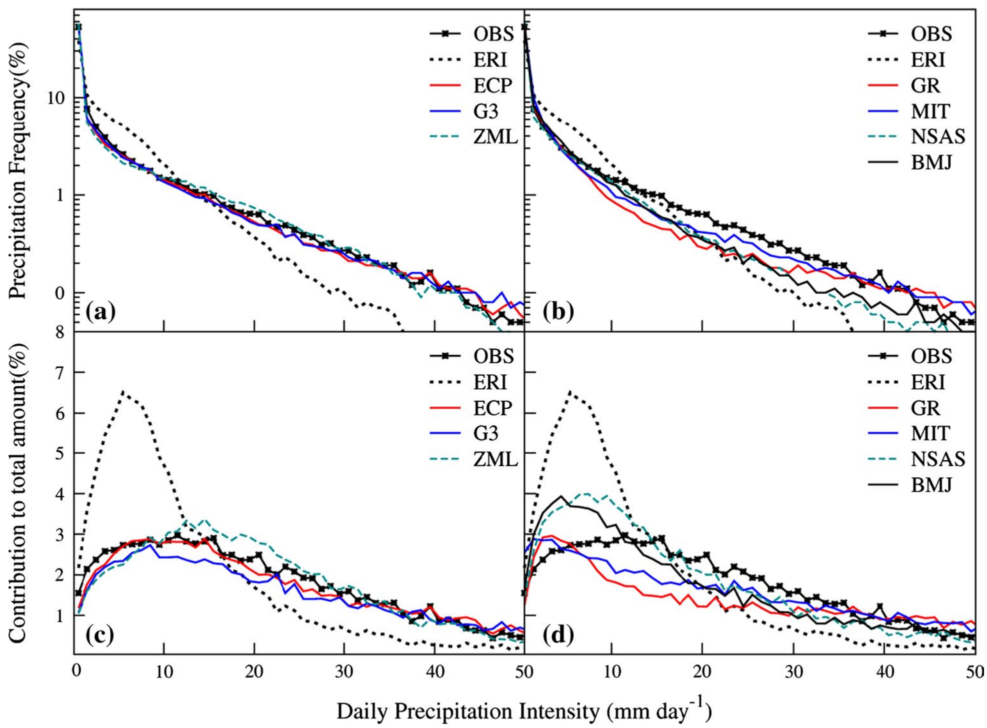

Fig. 4 Frequency distributions (**a**, **b**, in logarithm scales) of 1993 summer daily precipitation and the relative contribution to total amount (**c**, **d**) from each unit binned precipitation (1 mm day^{-1}) for all grids over the Central US as observed (OBS), and simulated by the CWRF using seven different cumulus schemes (ECP, G3, ZML, GR, MIT, NSAS, BMJ)

occurrence. Among them, the ECP scheme accurately predicts the relative contribution of daily rainfall intensity within the medium range (10–30 mm day-1) than the other two schemes. The other group, including GR, MIT, NSAS and BMJ, generally underestimates the frequency of heavy rainfall events and overestimates the contribution from light (GR and MIT) to medium (NSAS and BMJ) events.

Therefore, the ECP scheme not only well simulates the summer mean precipitation amount and daily variation, but also shows a clear superiority in reproducing the daily rainfall frequency distribution over the Central US. The cumulus closure assumption fundamentally determines the convection intensity and location (Grell and Dévényi 2002), the result also confirms that the moisture convergence assumption primarily contributes to the success of the ECP scheme in capturing the summer mean and daily precipitation variations over the Central US.

6 Precipitation diurnal cycle

Figure 5 illustrates the summer mean precipitation diurnal cycles for both 1993 and 2008 cases averaged over the Central US simulated by CWRF using the seven CUP schemes compared with NARR as the observational proxy. Following Liang et al. (2004b), the 3-hourly data from both NARR and CWRF are interpolated into hourly values by utilizing the spline fit method. To enhance the compatibility between observations and model simulations regarding the amplitude and phase of diurnal variations, the hourly rainfall amounts at each grid are normalized by a division of its daily mean values. The observed diurnal cycles for both cases exhibit a daytime minimum and a nighttime maximum but slightly differ in amplitude and phase. In NARR, the 1993 summer mean diurnal cycle has larger amplitude and the nocturnal rainfall peak occurs in the early morning at around 3–6 AM local solar time (LST), which is several hours later than that in the 2008 case. The diurnal cycle simulated by the seven CUP schemes are compared separately for the two groups as classified by the ability in predicting daily rainfall frequency distribution. The first group, including ECP, G3 and ZML, systematically generates a diurnal cycle with the peak locked at 15–18 PM LST, all failed to capture the observed nocturnal rainfall maxima. Among them, the ZML scheme tends to produce too large diurnal amplitudes, while the ECP and G3 exhibit similar but relatively smaller diurnal variations than observations.

In the second group, the GR and NSAS schemes are able to capture the diurnal timing, whereas the MIT and BMJ schemes unfaithfully produce rainfall maxima at early to late afternoon. This is in good agreement with previous findings by Liang et al. (2004a) and Lee et al. (2008). However, the NSAS scheme largely underestimates the peak amount and shows a tendency to rain earlier than observations particularly in 1993 summer. It is encouraging that the GR scheme, consistently with both CWRF and CMM5 (Liang et al. 2001), most realistically reproduces the diurnal amplitude and phase, albeit underestimating

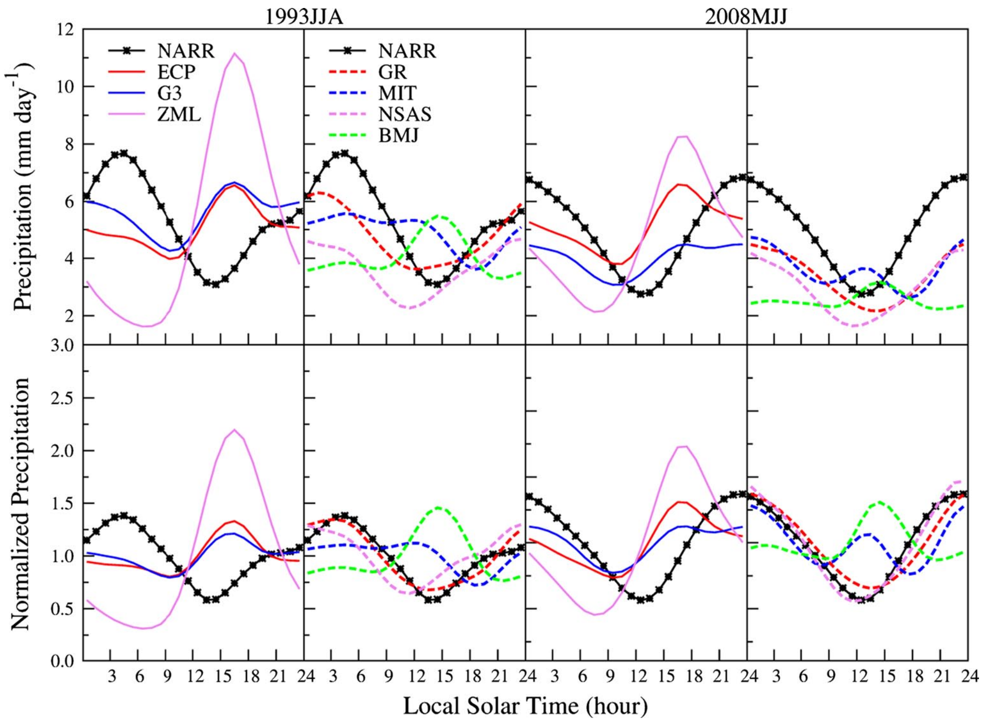

Fig. 5 Mean diurnal evolution (relative to local solar time) of hourly (mm day^{-1}, *upper panels*) and normalized hourly rainfall (*bottom panels*) averaged over the Central US for 1993 JJA (June–August) and 2008 MJJ (May–July) simulated by the CWRF using seven different cumulus schemes (ECP, G3, ZML, GR, MIT, NSAS, BMJ) compared with the NARR

the nocturnal rainfall peak amount. As such, the following focus on the GR scheme and attempt to explore the role of CUP in regulating the diurnal cycle over the Central US.

Figure 6 compares the 1993 summer mean rainfall diurnal cycles over the Central US from NARR and CWRF simulations using the GCE microphysical scheme but with or without the GR cumulus scheme. When cumulus parameterization is excluded, the CWRF only with the GCE microphysical scheme tends to produce a much stronger rainfall peak in the late evening at around 21 PM LST which is 6 h earlier than the observation. This earlier rainfall peak can be attributed to that the microphysical scheme over the Central US is more responsive to the large-scale dynamic forcing such as the Great Plain low-level jet whose strongest intensity generally leads the rainfall maxima for several hours (Liang et al. 2001; Lee et al. 2007a). By adding the GR cumulus scheme, this late evening peak amount is substantially reduced and the rainfall maximum is delayed to occur at the following early morning around 03-06 AM LST in better agreement with the observation. This improvement indicates that the cumulus parameterization plays an essential role in regulating the Central US precipitation diurnal cycle.

It is known that precipitation in the model is determined by the sub-grid convective and large-scale resolved (stratiform) components which are separately produced by CUP and explicit microphysical schemes. Previous studies (Lee et al. 2007b) found that models with less convective but more stratiform precipitation generate more nocturnal rainfall over the Central US. It is thus important to examine the role of stratiform precipitation in determining the Central US diurnal cycle.

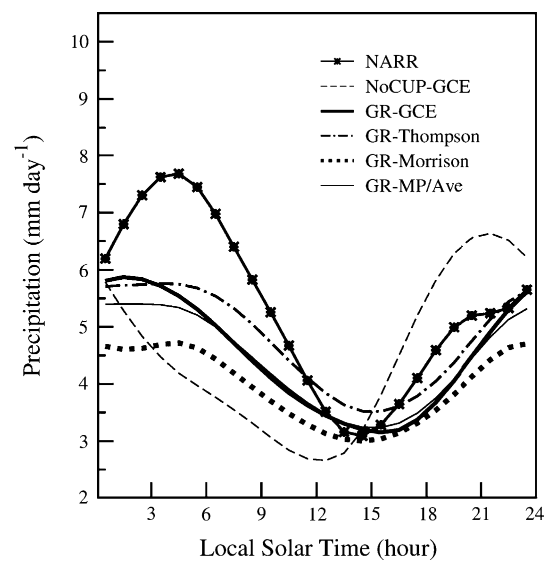

Fig. 6 1993 summer mean diurnal evolution (relative to local solar time) of (mm day^{-1}) rainfall averaged over the Central US simulated by the CWRF using the Grell cumulus scheme with three different microphysics including the Goddard Cumulus Ensemble (GR-GCE), the New Thompson (GR-Thompson), the Morrison (GR-Morrison) schemes and the averages from these three microphysics schemes (GR-MP/Ave), as compared to the simulation without the Grell cumulus scheme (NoCUP-GCE) and the NARR as observation

To examine the sensitivity of simulated diurnal cycle to the resolved precipitation, additional experiments are also

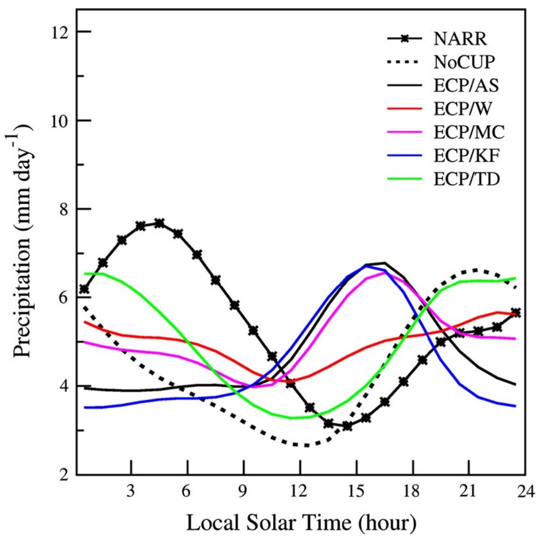

Fig. 7 1993 summer mean precipitation diurnal cycle (mm day^{-1}, local solar time) averaged over the Central US as observed (NARR) and simulated by the CWRF using the ECP scheme with five different closures (ECP/AS, ECP/W, ECP/MC, ECP/KF, ECP/TD) compared to the simulation without cumulus parameterization (NoCUP)

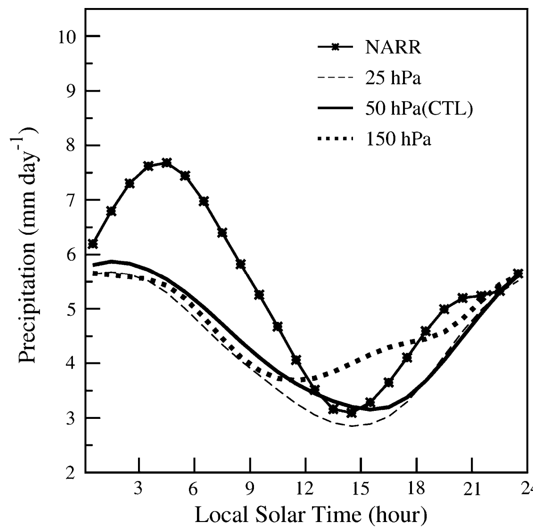

Fig. 8 1993 summer mean precipitation diurnal cycle (mm day^{-1}, local solar time) averaged over the Central US as observed (NARR) and simulated by the CWRF using the Grell cumulus scheme with three different lifting depth triggers including 25, 50 hPa (CTL, control) and 150 hPa

conducted by using the GR cumulus scheme but with different microphysical processes including the New Thompson (Thompson et al. 2008) and Morrison (Morrison et al. 2009) scheme, compared to the GCE microphysics. These three experiments using the same GR cumulus scheme but different microphysics all well predict the diurnal timing but largely differ in diurnal amplitude and rainfall magnitude. Compared to GCE, the New Thompson and Morrison schemes both produce weaker amplitudes, while the Morrison scheme largely underestimates nocturnal rainfall amounts. The comparison shows that the large-scale precipitation primarily contributes to the rainfall peak amount and diurnal amplitude, but hardly affects the diurnal phase. On the other hand, the diurnal timing of model precipitation is insensitive to the choice of microphysical schemes, implying that the GR cumulus scheme has intrinsic advantages over other CUPs in representing the physical mechanisms that control the Central US precipitation diurnal variation.

As suggested by Liang et al. (2004a), the superiority of the GR scheme in realistically capturing the Central US nocturnal rainfall maxima is due to its closure assumption in which convection is largely determined by the large-scale tropospheric forcing. However, few studies explicitly investigated the isolated effects of closure assumption. Given that the ECP scheme has incorporated five widely-used cumulus closures, sensitivity studies using these individual closures can help identify the effects of closures in predicting the Central US rainfall diurnal cycle.

Figure 7 shows the 1993 summer mean precipitation diurnal cycles averaged over the Central US simulated by the CWRF using the ECP scheme with five different closures, and No CUP, compared to NARR. The ECP with the AS, MC or KF closure assumption generally fails in capturing the nighttime rainfall, but tends to produce a diurnal cycle with rainfall peak locked at 15 PM LST. The failure has also been identified in the cumulus parameterization of BMJ, default version of ECP and ZML schemes, which use the above three closures, respectively. However, when the TD closure is used, it significantly improves the diurnal cycle simulation by generating a rainfall peak at the early morning with intensified intensity compared to other closures. Also, the ECP scheme with the TD closure shifts the rainfall peak from late evening in the CWRF simulation without CUP (NoCUP) to around 03 AM LST, albeit with 3 h phase error. It corresponds well with the behavior of the GR scheme that uses the same instability tendency closure assumption (Liang et al. 2004a). The result suggests that the large-scale instability tendency assumption for CUP closure may capture the dominate mechanisms that regulate the diurnal variation of convection over the Central US.

In addition to the closure assumption, certain trigger function has also been suggested to affect the CUP ability in simulating of diurnal phase over the Central US. For instance, Lee et al. (2008) showed that the lifting depth trigger plays a key role to simulate the nocturnal rainfall peak in SAS. The lifting depth is defined as the distance between the cloud base and convective starting level that must be less than 150 hPa. Their study suggested that this trigger primarily favors the nighttime convection because the lifting depth criterion is easier to be satisfied when convective starting level is elevated above the nocturnal inversion at night. Sensitivity experiments using the GR scheme with three different values for lifting depth trigger are carried out to further examine the effect of this trigger function.

Figure 8 compares the 1993 summer mean diurnal cycle simulated by the GR scheme with three lifting depth triggers: 25, 50 (control) and 150 hPa. Shallower depth (25 hPa) trigger generally tends to suppress convection because it is too small to activate the convection. When the lifting depth is increased to 150 hPa, daytime convection especially during the early afternoon is significantly enhanced because the threshold depth is large enough to trigger deep convection even at the presence of strong convective inhibition energy. As such, the lifting depth trigger in the GR scheme also affects the Central US diurnal cycle by mainly suppressing the daytime convection.

Above comparison, therefore, suggests that cumulus closure and lifting trigger in the GR scheme play different roles in determining the Central US diurnal cycle. The cumulus closure predominately regulates the diurnal phase and nocturnal rainfall maxima, while the lifting trigger effectively inhibits the daytime convection.

7 Conclusions and discussions

This study comprehensively evaluates the relative performance of 12 popular CUP schemes in predicting summer precipitation over the Central US. Three key features are specifically examined including mean pattern distribution, daily rainfall frequency and precipitation diurnal cycle. The CUP schemes in this study include 6 original WRF schemes (BMJ, NKF, SAS, NSAS, TDK, G3) and 6 new schemes (ECP, ZML, CSU, GFDL, MIT, GR) that have been widely used in GCMs or RCMs. All of them are implemented as deep convection schemes and combined with the UW shallow CUP scheme in order to provide a consistent evaluation for the moist cumulus parameterization. In particular, the ECP scheme is developed from the ensemble cumulus parameterization of G3 scheme with numerous improvements on the closure choices and regional dependence. By applying the moisture convergence closure over land and large-scale cloud-base vertical velocity assumption over oceans, the ECP scheme has been identified with advantages over other closures by sensitivity experiments (Qiao and Liang 2014a, b) in predicting the overall summer rainfall over the US land and oceans.

Sensitivity experiments of CWRF separately using the 12 CUP schemes are carried out for 1993 and 2008 summer when both record floods occurred over the Central US. Results show that these CUP schemes have distinctive skills in predicting the US summer mean precipitation distribution, with strong regional dependence. Seven CUP schemes are identified with complementary regime dependences in predicting summer rainfall patterns and amounts. One group, including ECP, G3 and ZML schemes, show advantages over other schemes in reproducing the Central US floods location and amount, but has large model disparities in other US regions and the adjacent coastal oceans. Particularly, the ECP scheme well reproduces the Central US floods and greatly reduces the wet biases in the G3 and ZML schemes along the US coastal oceans. The second group, including BMJ, GR, MIT and NSAS schemes, well captures the US summer precipitation geographic distribution, but largely underestimates the rainfall amounts over the Central US.

Further comparison of daily rainfall statistics shows that ECP most realistically reproduces the regional mean daily variation and the overall frequency distribution of daily precipitation. It not only greatly reduces the deficiency of ERI reanalysis by better capturing the occurrence of heavy rainfall events, but also more accurately predicts the contributions from daily precipitation in medium intensity than the G3 and ZML. The other schemes that largely underestimate the Central US summer floods, generally failed to accurately predict the daily variation, except that NSAS well captures the temporal variation of daily rainfall but has large errors in predicting rainfall amounts.

Most CUP schemes fail in reproducing the observed nocturnal rainfall maxima over the Central US. An encouraging finding is the GR cumulus scheme is superior in reproducing the Central US diurnal amplitude and phase, though it still underestimates the nocturnal rainfall peak. The CWRF with only explicit microphysics schemes tend to have stronger but much earlier rainfall peaks, while the inclusion of GR cumulus scheme effectively regulates the diurnal phase by postponing the rainfall peak from late evening to early morning in a better alignment with observations. Moreover, the diurnal timing simulated by the GR cumulus scheme is found to be insensitive to the choice of microphysics schemes, implying that large-scale explicit precipitation primarily contributes to the nighttime rainfall peak but hardly affects the diurnal phase.

Replacing the moisture convergence closure in the ECP scheme with the large-scale instability tendency closure that is also used in the GR scheme greatly improves the ECP simulated diurnal cycle by generating a nocturnal rainfall peak. This suggests that the advantage of the GR scheme for capturing nocturnal rainfall maxima is primarily due to its closure assumption in which the convection is determined by the increase rate of large-scale instability. In addition, the lifting depth trigger in GR also affects the Central US diurnal cycle simulation by mainly suppressing the daytime convection, consistent with the study by Lee et al. (2008).

Although the ECP scheme with the moisture convergence closure over the land shows superiority in reproducing the Central US floods particularly regarding the geographic distributions and daily variations, it still overestimates the rainfall over the Southeast US and the North American Monsoon region. Several additional experiments (Qiao and Liang 2014a) have suggested that the wet biases over these two regions can be greatly reduced by using the cloud-base vertical velocity closure. These two closures thus in the ECP scheme complementarily capture the observed rainfall pattern over distinct regions. In Liang et al. (2007), an optimal ensemble based on two CUP schemes that have strong complementarity in simulating certain observed signals has produced a more skillful result overall regarding the interannual anomaly and climate mean. Given the known regime dependence of closure assumption in the ECP scheme, future work should be focused on deriving localized dynamic weighting for different closures to improve the summer mean prediction over the entire US.

Another important issue is the diurnal cycle simulation by the ECP scheme warrants further investigation. Above analyses have shown that the large-scale instability tendency closure mainly contributes the success of the GR cumulus scheme in reproducing the Central US diurnal phase and amplitude. Also the unrealistic afternoon rainfall peaks in the ECP scheme are greatly inhibited and the nocturnal rainfall maxima are generated when ECP uses this instability tendency closure rather than the defaulted moisture convergence closure assumption. The implication is that the rate of increase of large-scale instability plays a dominate role in regulating the diurnal variation of convection over the Central US Xie et al. (2004) implemented a convective trigger function that utilizes the large-scale instability tendency and effectively reduced the frequent occurrence of convection during the daytime, leading to considerable improvements in the overall US diurnal cycle simulation. As such, more efforts will be made to incorporate the large-scale tendency assumption as trigger function in the ECP scheme in order to improve the diurnal cycle simulation over the Central US.

In addition, this study has indicated that the CUP regulates the nocturnal diurnal timing over the Central US with important sensitivity to the closure assumptions and lifting-depth trigger function, while the microphysics schemes does not affect the timing but alter the magnitude of total precipitation. Thus, accurate predictions of summer rainfall may be achieved by optimizing the balance between CUP and microphysics representations.

Although various cumulus schemes have been developed to predict the convective precipitation and associated heat and moisture changes of the atmosphere, the CUP problem is far from being solved and remains among the challenges to the modeling community. They generally involved different physical assumptions that are not fully evaluated and tunable parameters whose actual value are unknown, leading to model deficiency and large uncertainty.

Specifically, there is no consensus yet on the closure assumptions for dynamic control in large-scale or mesoscale models. For the static control, great uncertainties exist in representing the complicated processes in clouds and their interactions with environment, including the entrainment/detrainment effects, microphysical process in cumulus clouds, and convective downdrafts (Randall et al. 2003). For the high-resolution mesoscale model, a set of additional trigger functions are often imposed to evaluate the possibility of convection initiation when closure conditions are not sufficient for predicting the occurrence of convection. Most triggers in current cumulus schemes are related to the accessibility of CAPE, or the probability to overcome the negative buoyancy below the level of free convection, but these triggers are highly variable and strongly case-dependent (Kain and Fritsch 1993).

Another important factor that warrants to be further examined is the model resolution. It is known to have impacts on the partition of the convective and stratiform rainfall amounts, and thus affect the rainfall diurnal cycle simulation. However, large uncertainty still existed about the model dependence upon the increasing resolution. Lee et al. (2007b) has examined the sensitivity of AGCM simulation of warm seasonal diurnal cycle of precipitation over the US to horizontal resolution. Their results showed that the phase of the diurnal cycle of precipitation is generally improved with increasing resolution (from approximately 2° to 1/2°), but large errors remain even at the highest resolution in their study (1/2°). They suggested that further improvements in cumulus parameterization are still required to reduce these errors, even though with higher model resolution.

Previous RCM studies used horizontal grids typically ranging in 60–30 km, while the GCM studies in 200–300 km. As the model resolution increases toward about 4 km or finer, the CUP can be eliminated in general. Such a cloud-resolving capability, although desirable, is computationally intensive and not affordable for long-term climate simulations in the near term. In addition, it is yet to prove that explicit representation of convection produces better forecasts than those using the CUP in mesoscale models. Therefore, the ECP scheme offers a framework for further improvements that are useful for mesoscale climate modeling studies.

Acknowledgments We thank Dr. Georg Grell for developing, and providing guidance on the application of the G3 scheme which forms the basis of the ECP scheme in the CWRF. We are also appreciative of Tiejun Ling, Min Xu and Shenjian Su for helping with CWRF post processing job scripts. This research was supported by the NOAA Education Partnership Program (EPP) COM Howard 631017, the Climate Prediction Program for the Americas (CPPA) NA08OAR4310575 and NA08OAR4310875, and Project 44505880/004 in East China Normal University. The model simulations were conducted at the NOAA/ESRL and UIUC/NCSA facilities. The views expressed are those of the authors and do not necessarily reflect those of the sponsoring agencies.

Appendix 1

Cumulus parameterizations

All deep and shallow cumulus schemes in CWRF are mass-flux based parameterizations, in which different closure assumptions are used to determine the cloud base mass flux by linking the existence and intensity of convection to large-scale processes. According to closure assumptions, all schemes are divided into three major groups and their associated features are briefly summarized below.

Multiple closure schemes

The GD, G3, and ECP schemes are all ensemble mass-flux type schemes with multiple closure assumptions and variants of parameters in the static control including updraft and downdraft entrainment and detrainment and precipitation efficiency. The GD scheme was first introduced by Grell and Dévényi (2002) in which the dynamic control closures are based on convective available potential energy or cloud work function, low-level vertical velocity, or integrated vertical advection of moisture. The G3 scheme is developed on the basis of the GD scheme, but excludes the quasi-equilibrium assumption from closure ensemble members. The ECP scheme is modified from the G3 scheme but with numerous improvements by primarily adding relative weights for different dynamic closures and including regional dependence between the land and ocean. The ECP scheme includes five major closures to determine the cloud base mass flux. The AS closure (Arakawa and Schubert 1974) assumes an instantaneous equilibrium between the large scale forcing and the convection by relaxing the cloud work function toward a climatological value. The W closure (Brown 1979; Frank and Cohen 1987) assumes that net cloud base mass flux is determined by environmental mass flux averaged from the surrounding nine points at lower tropospheric levels such as cloud base or updraft originating level. The MC closure (Krishnamurti et al. 1983) is the widely-used moisture convergence assumption in which convection develops to balance the column integrated moisture convergence. The KF closure is based on Kain and Fritsch (1993) assumption in which the convection acts to reduce the CAPE towards zero over a specific time scale (around 40 min in the ECP scheme). The TD closure is also based on the quasi-equilibrium assumption but determines the convection by the increase rate of large-scale instability (Grell 1993). In the current ECP scheme, the moisture convergence and averaged cloud-base vertical velocity closure is separately implemented over land and oceans.

Total instability adjustment schemes

Three CUPs (ZML, NKF, TDK) are based on the total instability adjustment closure assumption in which the convection acts to reduce the CAPE towards zero over a specific time scale. The ZML is the parameterization of Zhang and McFarlane (1995) with modifications to facilitate its application in high resolution models for deep convection (Liang et al. 2012). The moist convection occurs only when the local atmosphere is conditionally unstable in the lower troposphere. The updraft ensemble is only comprised of those plumes which can penetrate through this convective layer and these updrafts are assumed to have same initial upward mass fluxes from the sub-cloud layer to simplify the formulations.

The NKF scheme (Kain 2004) is a modified version of Kain and Fritsch (1993). It utilizes a one-dimensional cloud model with explicitly representation of effects of moist updrafts and downdrafts, the entrainment, detrainment and simple microphysics involved. This scheme triggers the convection when the net column convective instability is present and the parcel temperature is higher than the environmental value. To induce stronger convection in the presence of the large-scale upward motion, a perturbation to the parcel temperature which is proportional to the grid-scale vertical motion at the lifting condensation level is incorporated as an additional trigger function. The TDK scheme is originally designed by Tiedtke (1989) and revised by Nordeng (1995). It is a bulk mass flux model based on the CAPE removal closure. The convection is activated when the moisture convergence is greater than a limit of boundary layer turbulent moisture flux. This scheme considers three types of convection: (1) deep convection that occurs under disturbed, conditionally unstable conditions in the presence of lower tropospheric large-scale moisture convergence; (2) shallow convection that occurs in a suppressed environment and is mainly driven by the turbulent surface moisture flux; (3) mid-level convection that occurs mainly in conditional unstable condition, but with the cloud base above the PBL.

Quasi-equilibrium closure-based schemes

The remaining eight schemes (BMJ, GR, MIT, GFDL, SAS, NSAS, CSU, and UW) are all established on the QE closure assumption but with alterations. The BMJ scheme is a moist adjustment parameterization developed by Betts (1986) and Betts and Miller (1986), and modified by Janjic (1994) for both deep and shallow convection. It assumes that the profiles of temperature and moisture in a column with sufficient resolved-scale vertical motion and instability are instantaneously relaxed toward to observed neutral structures. It does not explicitly represent the subgrid updrafts and downdrafts and the mesoscale microphysical processes.

The GR scheme is proposed by Grell (1993) as a simplified mass flux scheme that only consists of a single pair of updraft and downdraft without direct mixing between them. Convection in this scheme is determined by the rate of destabilization in which the change of instability due to convection balances the changes due to nonconvective effects. The convection is not activated until a lifting depth criterion is met.

The MIT scheme is the parameterization of Emanuel (1991) and Emanuel and Živković-Rothman (1999). The closure employs a subcloud-layer quasi-equilibrium hypothesis (Raymond 1995) which states that convective mass fluxes will adjust so that air within the subcloud layer remains neutrally buoyant with respect to upward displacements to just above the top of the subcloud layer. It utilizes the buoyance-sorting assumption of Raymond and Blyth (1986) which assumes that mixing in clouds is highly episodic, rather than continuous as in the entraining plume model. Convection occurs whenever the environment is unstable to a parcel in reversible adiabatic ascent from the surface.

The GFDL scheme is the parameterization developed by Donner (1993) as implemented by Donner et al. (2001). The convection is triggered when the large-scale CAPE generation rate is positive and the maximum convective inhibition cannot exceed 10 J Kg^{-1}. This scheme is unique in that it augments cloud base mass flux with convective-scale vertical velocities to include the microphysics of mesoscale anvils, leading to a consistent interaction between convection, microphysics and radiation.

The SAS scheme is a simplified version of Arakawa and Schubert (1974) scheme developed by Pan and Wu (1995). It determines the cloud base mass flux by relaxing the cloud work function to a critical value over a fixed timescale. To trigger the convection, this critical value must be exceeded and is assumed to be a function of the cloud base vertical motion. As such, the critical value is allowed to approach zero as the large-scale rising motion becomes strong. This scheme also defines the upper limit of convective inhibition using the lifting depth trigger in which the depth between the parcel originating level and level of free convection must be less than 150 hPa.

The NSAS scheme is based on the SAS scheme but with several modifications to trigger functions. For instance, the fixed value of lifting depth trigger (150 hPa) is changed to vary within the range of 120–180 hPa, in proportional to the cloud base grid-scale vertical velocity. This intends to produce more convection in large-scale convergence regions but less convection in subsidence areas (Han and Pan 2011).

The CSU scheme is the parameterization of Arakawa and Schubert (1974) but with a prognostic cumulus kinetic energy (CKE) closure (Pan and Randall 1998) and interactive liquid and ice cloud microphysics (Fowler and Randall 2002). This prognostic closure relaxes the quasi-equilibrium assumption by explicitly predicting the CKE for each cumulus subensemble. The cloud-base mass flux is determined by the CKE and a dimensional parameter (α) which is related to the adjustment time defined by original Quasi-equilibrium assumption. In current version of CSU scheme, a constant value of α (10^8) is given for all cloud types.

The UW scheme is a bulk mass-flux based shallow cumulus parameterization of Bretherton and Park (2009) in which entrainment and detrainment is derived using a buoyancy-sorting algorithm. This scheme has a combined closure and trigger based on convective inhibition. It assumes that shallow convection can only form if the source air has sufficient vertical velocity to penetrate the weak inversion at the top of subcloud layer and reach its level of free convection. The cloud base mass flux is determined as to maintain dynamical equilibrium between the subcloud turbulent boundary layer and the base of cumulus cloud layer.

Appendix 2

Three microphysics schemes

The Goddard Cumulus Ensemble (GCE) model (Tao et al. 2003), the New Thompson (Thompson et al. 2008), and the Morrison et al. (2009) scheme are compared to examine the sensitivity of summer precipitation diurnal cycle predictions to large-scale microphysics. All three microphysics parameterizations are mixed-phased schemes, including six classes of water substances: water vapor, cloud water, rain, cloud ice, snow and graupel.

The GCE scheme is one-moment bulk microphysical schemes based on Lin et al. (1983) with several modifications. They include the prognostic equations for mixing ratios of cloud hydrometers, the options to choose either graupel (low density and high number concentration) or hail (high density and low number concentration), and the instantaneous adjustment for saturation computation to evaluate evaporation of rain and deposition or sublimation of snow/graupel/hail.

The New Thompson scheme is greatly improved compared to one-moment scheme by including a two-moment prognostic scheme for cloud ice. Differing from the GCE scheme, it assumes a generalized gamma distribution for all species instead of purely exponential distribution.

However, the Morrison scheme is a two-moment microphysical scheme. The prognostic variables are number concentrations and mixing ratios of six water species whose particle size distributions are represented as gamma distributions.

References

Anderson CJ, Arritt RW, Pan Z, Takle ES, Gutowski WJ, Otieno FO, da Silva R, Caya D, Christensen JH, Lüthi D, Gaertner MA, Gallardo C, Giorgi F, Laprise R, Hong S-Y, Jones C, Juang H-MH, Katzfey JJ, McGregor JL, Lapenta WM, Larson JW, Taylor JA, Liston GE, Pielke RA, Roads JO (2003) Hydrological processes in regional climate model simulations of the central United States flood of June–July 1993. J Hydrometeorol 4:584–598

Arakawa A, Schubert WH (1974) Interaction of a cumulus cloud ensemble with the large-scale environment, part I. J Atmos Sci 31:674–701

Becker EJ, Berbery EH (2008) The diurnal cycle of precipitation over the North American Monsoon Region during the NAME 2004 field Campaign. J Clim 21:771–787

Beljaars ACM, Viterbo P, Miller MJ, Betts AK (1996) The anomalous rainfall over the United States during July 1993: sensitivity to land surface parameterization and soil moisture anomalies. Mon Weather Rev 124:362–383

Bell GD, Janowiak JE (1995) Atmospheric circulation associated with the midwest floods of 1993. Bull Am Meteorol Soc 76:681–695

Betts AK (1986) A new convective adjustment scheme. Part I: observational and theoretical basis. Quart J R Meteorol Soc 112:677–691

Betts AK, Miller MJ (1986) A new convective adjustment scheme. Part II: single column tests using GATE wave, BOMEX, and arctic air-mass data sets. Quart J R Meteorol Soc 112:693–709

Bosilovich MG, Sun W (1999) Numerical simulation of the 1993 midwestern flood: land–atmosphere interactions. J Clim 12:1490–1505

Bretherton CS, Park S (2009) A new moist turbulence parameterization in the community atmosphere model. J Clim 22:3422–3448

Brown JM (1979) Mesoscale unsaturated downdrafts driven by rainfall evaporation: a numerical study. J Atmos Sci 36:313–338

Chen M, Shi W, Xie P, Silva VBS, Kousky VE, Higgins RW, Janowiak JE (2008) Assessing objective techniques for gauge-based analyses of global daily precipitation. J Geophys Res 113:D04110. doi:10.1029/2007JD009132

Choi HI, Liang X-Z (2010) Improved terrestrial hydrologic representation in mesoscale land surface models. J Hydrometeorol 11:797–809

Choi HI, Kumar P, Liang X-Z (2007) Three-dimensional volume-averaged soil moisture transport model with a scalable parameterization of subgrid topographic variability. Water Resour Res 43:W04414. doi:10.1029/2006WR005134

Choi HI, Liang X-Z, Kumar P (2013) A conjunctive surface-subsurface flow representation for mesoscale land surface models. J Hydrometeorol 14:1421–1442

Chou M-D, Suarez MJ (1999) A solar radiation parameterization for atmospheric studies. [Last revision on 10.1007/s00382-014-2301-7 March 2002]. In: Suarez MJ (ed) Technical report series on global modeling and data assimilation, NASA/TM-1999-104606, vol 15. Goddard Space Flight Center, Greenbelt, MD

Chou M-D, Suarez MJ, Liang X-Z, Yan M M-H (2001) A thermal infrared radiation parameterization for atmospheric studies. [Last revision on July 2002]. In: Suarez MJ (ed)Technical report series on global modeling and data assimilation. NASA/TM-2001-104606, vol 19. Goddard Space Flight Center, Greenbelt, MD

Coleman JSM, Budikova D (2010) Atmospheric aspects of the 2008 Midwest floods: a repeat of 1993? Int J Climatol 30:1645–1667. doi:10.1002/joc.2009

Dai A (1999) Recent changes in the diurnal cycle of precipitation over the United States. Geophys Res Lett 26:341–344

Daly C, Halbleib M, Smith JI, Gibson WP, Doggett MK, Taylor GH, Curtis J, Pasteris PA (2008) Physiographically-sensitive mapping of temperature and precipitation across the conterminous United States. Int J Climatol 28:2031–2064

Davis CA, Manning KW, Carbone RE, Trier SB, Tuttle JD (2003) Coherence of warm-season continental rainfall in numerical weather prediction models. Mon Weather Rev 131:2667–2679

Dirmeyer PA, Kinter JL (2010) Floods over the U.S. midwest: a regional water cycle perspective. J Hydrometeorol 11:1172–1181. doi:10.1175/2010JHM1196.1

Donner LJ (1993) A cumulus parameterization including mass fluxes, vertical momentum dynamics, and mesoscale effects. J Atmos Sci 50:889–906

Donner L, Seman CJ, Hemler RS, Fan S (2001) A cumulus parameterization including mass fluxes, convective vertical velocities, and mesoscale effects: thermodynamic and hydrological aspects in a general circulation model. J Clim 14:3444–3463

Emanuel KA (1991) A scheme for representing cumulus convection in Large-Scale models. J Atmos Sci 48:2313–2335

Emanuel KA, Živković-Rothman M (1999) Development and evaluation of a convection scheme for use in climate models. J Atmos Sci 56:1766–1782

Fowler LD, Randall DA (2002) Interactions between cloud microphysics and cumulus convection in the CSU general circulation model. J Atmos Sci 59:3074–3098

Frank WM, Cohen C (1987) Simulation of tropical convective systems. Part I: a cumulus parameterization. J Atmos Sci 44:3787–3799

Grell GA (1993) Prognostic evaluation of assumptions used by cumulus parameterizations. Mon Weather Rev 121:764–787

Grell GA, Dévényi D (2002) A generalized approach to parameterizing convection combining ensemble and data assimilation techniques. Geophys Res Lett 29:14.doi:10.1029/2002GL015311

Groisman PY, Knight RW, Karl TR (2012) Changes in intense precipitation over the Central United States. J Hydrometeorol 13:47–66

Han J, Pan H-L (2011) Revision of convection and vertical diffusion schemes in the NCEP global forecast system. Weather Forecast 26:520–533

Janjic ZI (1994) The step-mountain eta coordinate model: further developments of the convection, viscous sublayer and turbulence closure schemes. Mon Weather Rev 122:927–945

Jiang X, Lau N-C, Klein SA (2006) Role of eastward propagating convection systems in the diurnal cycle and seasonal mean of summertime rainfall over the U.S. Great Plains. Geophys Res Lett 33:L19809. doi:10.1029/2006GL027022

Kahn RA, Garay MJ, Nelson DL, Yau KK, Bull MA, Gaitley BJ, Martonchik JV, Levy RC (2007) Satellite-derived aerosol optical depth over dark water from MISR and MODIS: comparisons with AERONET and implications for climatological studies. J Geophys Res 112:D18205. doi:10.1029/2006JD008175

Kain JS (2004) The Kain-Fritsch convective parameterization: an update. J Appl Meteorol 43:170–181

Kain JS, Fritsch JM (1993) Convective parameterization for mesoscale models: the Kain-Fritcsh scheme. In: Emanuel KA, Raymond DJ (eds) The representation of cumulus convection in numerical models. American Meteorology Society, 246 pp

Karl TR, Knight RW (1998) Secular trends of precipitation amount, frequency, and intensity in the United States. Bull Am Meteorol Soc 79:231–241

Krishnamurti TN, Low-Nam S, Pasch R (1983) Cumulus parameterization and rainfall rates II. Mon Weather Rev 111:815–828
Kunkel KE, Changnon SA, Angel JR (1994) Climatic aspects of the 1993 upper Mississippi river basin flood. Bull Am Meteorol Soc 75:811–822
Kunkel KE, Easterling DR, Redmond K, Hubbard K (2003) Temporal variations of extreme precipitation events in the United States: 1895–2000. Geophys Res Lett 30:17. doi:10.1029/2003GL018052
Liang X-Z, Wang W-C, Boyle JS (1997) Atmospheric ozone climatology for use in general circulation models. PCMDI Report No 43, UCRL-MI-125650
Liang X-Z, Xu M, Gao W, Kunkel KE, Slusser J, Dai Y, Min Q, Houser PR, Rodell M, Schaaf CB, Gao F (2005) Development of land surface albedo parameterization bases on moderate resolution imaging spectroradiometer (MODIS) data. J Geophys Res 110:D11107. doi:10.1029/2004JD005579
Lee M-I, Schubert SD, Suarez MJ et al (2007a) An analysis of the warm-season diurnal cycle over the continental United States and northern Mexico in general circulation models. J Hydrometeorol 8:344–366
Lee M-I, Schubert SD, Suarez MJ et al (2007b) Sensitivity to horizontal resolution in the AGCM simulations of warm season diurnal cycle of precipitation over the United States and Northern Mexico. J Clim 20:1862–1881
Lee M-I, Schubert SD, Suarez MJ, Schemm J-K E, Pan H-L, Han J, Yoo S-H (2008) Role of convection triggers in the simulation of the diurnal cycle of precipitation over the United States Great Plains in a general circulation model. J Geophys Res 113:D02111, doi:10.1029/2007JD008984
Liang X-Z, Zhang F (2013) The cloud-aerosol-radiation (CAR) ensemble modeling system. Atmos Chem Phys 13:8335–8364. doi:10.5194/acp-13-8335-2013
Liang X-Z, Kunkel KE, Samel AN (2001) Development of a regional climate model for U.S. midwest applications. Part I: sensitivity to buffer zone treatment. J Clim 14:4363–4378
Liang X-Z, Li L, Dai A, Kunkel KE (2004a) Regional climate model simulation of summer precipitation diurnal cycle over the United States. Geophys Res Lett 31. doi:10.1029/2004GL021054
Liang X-Z, Li L, Kunkel KE, Ting M, Wang JXL (2004b) Regional climate model simulation of U.S. Precipitation during 1982–2002. Part I: annual cycle. J Clim 17:3510–3529
Liang X-Z, Pan J, Zhu J, Kunkel KE, Wang JXL, Dai A (2006) Regional climate model downscaling of the U.S. summer climate and future change. J Geophys Res 111:D10108. doi:10.1029/2005JD006685
Liang X-Z, Xu M, Kunkel KE, Grell GA, Kain J (2007) Regional climate model simulation of U.S.-Mexico summer precipitation using the optimal ensemble of two cumulus parameterizations. J Clim 20:5201–5207
Liang X-Z, Xu M, Yuan X, Ling T, Choi HI, Zhang F, Chen L, Liu S, Su S, Qiao F, He Y, Wang JXL, Kunkel KE, Gao W, Joseph E, Morris V, Yu T-W, Dudhia J, Michalakes J (2012) Regional climate-weather research and forecasting model (CWRF). Bull Am Meteorol Soc 120404072510007. doi:10.1175/BAMS-D-11-00180.1
Lin Y-L, Farley RD, Orville HD (1983) Bulk parameterization of the snow field in a cloud model. J Clim Appl Meteorol 22:1065–1092
Mesinger F, DiMego G, Kalnay E et al (2006) North American regional reanalysis. Bull Am Meteorol Soc 87:343–360
Mo KC, Paegle JN, Higgins RW (1997) Atmospheric processes associated with summer floods and droughts in the Central United States. J Clim 10:3028–3046
Morrison H, Thompson G, Tatarskii V (2009) Impact of cloud microphysics on the development of trailing stratiform precipitation in a simulated squall line: comparison of one- and two-moment schemes. Mon Weather Rev 137:991–1007
Nakamura J, Lall U, Kushnir Y, Robertson AW, Seager R (2013) Dynamical structure of extreme floods in the US Midwest and the United Kingdom. J Hydrometeorol 14:485–504
Nordeng TE (1995) Extended version of the convective parameterization scheme at ECMWF and their impact on the mean and transient activity of the model in the Tropics. ECMWF Research Department Tech. Memo. 2006, 41 pp
Paegle J, Mo KC, Nogués-Paegle J (1996) Dependence of simulated precipitation on surface evaporation during the 1993 United States summer floods. Mon Weather Rev 124:345–361
Pan D-M, Randall DA (1998) A cumulus parameterization with a prognostic closure. Quart J R Meteorol Soc 124:949–981
Pan H-L, Wu W-S (1995) Implementing a mass flux convection parameterization package for the NMC medium-range forecast model, NMC Office Note, 409, 40 pp, National Centre for Environment Prediction, CampSprings, MD
Qiao F, Liang X-Z (2014a) Effects of cumulus parameterization closures on summer precipitation prediction over the United States coastal oceans. J Clim (submitted)
Qiao F, Liang X-Z (2014b) Effects of cumulus parameterization closures on summer precipitation prediction over the continental United States. J Clim (submitted)
Randall D, Khairoutdinov M, Arakawa A, Grabowski W (2003) Breaking the cloud parameterization deadlock. Bull Am Meteorol Soc 84:1547–1564
Raymond DJ (1995) Regulation of moist convection over the west Pacific warm pool. J Atmos Sci 52:3945–3959
Raymond DJ, Blyth AM (1986) A stochastic mixing model for non-precipitating cumulus clouds. J Atmos Sci 43:2708–2718
Skamarock WC, Klemp JB, Dudhia J, Gill DO, Barker DM, Duda MG, Huang X-Y, Wang W, Powers JG (2008) A description of the advanced research WRF Version 3. NCAR Technical Note, NCAR/TN-475 + STR, 113 pp
Smith JA, Baeck ML, Villarini G, Wright DB, Krajewski W (2013) Extreme flood response: the June 2008 flooding in Iowa. J Hydrometeorol 14:1810–1825
Takle ES, Gutowski WJ Jr, Arritt RW, Pan Z, Anderson CJ, da Silva RR, Caya D, Chen S-C, Giorgi F, Christensen JH, Hong S-Y, Juang H-MH, Katzfey J, Lapenta WM, Laprise R, Listen GE, Lopez P, McGregor J, Pielke RA Sr, Roads JO (1999) Project to intercompare regional climate simulations (PIRCS): description and initial results. J Geophys Res 104:19443–19461
Tao WK, Simpson J, Baker D, Braun S, Chou MD, Ferrier B, Johnson D, Khain A, Lang S, Lynn B (2003) Microphysics, radiation and surface processes in the Goddard cumulus ensemble (GCE) model. Meteorol Atmos Phys 82:97–137
Taylor KE (2001) Summarizing multiple aspects of model performance in a single diagram. J Geophys Res Atmos 106:7183–7192
Thompson G, Field PR, Rasmussen RM, Hall WD (2008) Explicit forecasts of winter precipitation using an improved bulk microphysics scheme. Part II: implementation of a new snow parameterization. Mon Weather Rev 136:5095–5115
Tiedtke M (1989) A comprehensive mass flux scheme for cumulus parameterization in large-scale models. Mon Weather Rev 117:1779–1800
Ting M, Wang H (2006) The role of the North American topography on the maintenance of the great plains summer low-level jet. J Atmos Sci 63:1056–1068. doi:10.1175/JAS3664.1
Trenberth KE, Dai A, Rasmussen RM, Parsons DB (2003) The changing character of precipitation. Bull Am Meteorol Soc 84:1205–1217
Uppala SM, Dee DP, Kobayashi S, Berrisford P, Simmons AJ (2008) Towards a climate data assimilation system: status update of ERA-Interim. ECMWF Newsl 115:12–18
Villarini G, Smith JA, Baeck ML, Vitolo R, Stephenson DB, Krajewski WF (2011) On the frequency of heavy rainfall for the Midwest of the United States. J Hydrol 400:103–120

Xie P, Arkin PA (1997) Global precipitation: a 17-year monthly analysis based on gauge observations, satellite estimates, and numerical model outputs. Bull Am Meteorol Soc 78:2539–2558

Xie S, Zhang M, Boyle JS, Cederwall RT, Potter GL, Lin W (2004) Impact of a revised convective triggering mechanism on Community Atmosphere Model, Version 2, simulations: results from short-range weather forecasts. J Geophys Res 109:D14102. doi:10.1029/2004JD004692

Xu K-M, Randall DA (1996) A semiempirical cloudiness parameterization for use in climate models. J Atmos Sci 53:3084–3102

Yuan X, Liang X-Z (2011) Evaluation of a conjunctive surface-subsurface process model (CCSP) over the contiguous United States at regional-local scales. J Hydrometeorol 12:579–599. doi:10.1175/2010JHM1302.1

Zhang GJ, McFarlane NA (1995) Sensitivity of climate simulations to the parameterization of cumulus convection in the Canadian Climate Centre general circulation model. Atmos Ocean 33:407–446